Effects of photon statistics in wave mixing on a single qubit

W. V. Pogosov,[1,2] A. Yu. Dmitriev,[3,4] and O. V. Astafiev[5,3,6,7]
[1]*Dukhov Research Institute of Automatics (VNIIA), 127055 Moscow, Russia*
[2]*Institute for Theoretical and Applied Electrodynamics, Russian Academy of Sciences, 125412 Moscow, Russia*
[3]*Laboratory of Artificial Quantum Systems, Moscow Institute of Physics and Technology, 141700 Dolgoprudny, Russia*
[4]*National University of Science and Technology MISIS, Moscow 119049, Russia*
[5]*Skolkovo Institute of Science and Technology, 121205 Moscow, Russia*
[6]*Physics Department, Royal Holloway, University of London, Egham, Surrey TW20 0EX, United Kingdom*
[7]*National Physical Laboratory, Teddington TW11 0LW, United Kingdom*

(Received 26 February 2021; accepted 22 July 2021; published 5 August 2021; corrected 9 December 2021)

We theoretically consider wave mixing under the irradiation of a single qubit by two photon fields. The first signal is a classical monochromatic drive, while the second one is a nonclassical light. Particularly, we address two examples of a nonclassical light: (i) a broadband squeezed light and (ii) a periodically excited quantum superposition of Fock states with 0 and 1 photons. The mixing of classical and nonclassical photon fields gives rise to side peaks due to the elastic multiphoton scattering. We show that a side peaks structure is distinct from the situation when two classical fields are mixed. The most striking feature is that some peaks are absent. The analysis of peak amplitudes can be used to probe photon statistics in the nonclassical mode.

DOI: 10.1103/PhysRevA.104.023703

I. INTRODUCTION

Wave mixing is a well-known phenomenon in the domain of nonlinear optics that has various applications [1–3]. This effect manifests itself in a generation of waves with new frequencies as a result of interaction between incoming two or three frequency waves, which conserves the total energy of the photons. Wave mixing occurs in a nonlinear medium characterized by nonzero second-order or higher-order susceptibilities [2].

Recent progress in microfabrication methods and quantum fields control has resulted in the possibility to realize nonlinear effects on the level of a single artificial quantum system. Progress in this direction is of importance in the context of quantum information processing. One of the promising platforms for the construction of quantum devices is superconducting quantum circuits. Particularly, superconducting systems offer regimes which are not accessible for natural atoms and give rise to various unusual quantum optics phenomena, both in on-chip and open-space configurations; see, e.g., Refs. [4–14]. An example of such a phenomena is a wave mixing on a single artificial atom that was demonstrated experimentally in the series of articles [15–17]. The atom plays a role of a nonlinear element providing interaction between microwaves. In Ref. [17], wave mixing of continuous coherent waves on a superconducting flux qubit coupled to the coplanar waveguide was demonstrated and the existence of narrow side peaks of different orders in nonlinearity was observed, which have been attributed to elastic multiphoton scattering. Although both the experimental and theoretical results of Ref. [17] were obtained for coherent waves only, it was suggested that the amplitudes of side peaks, in general, should be sensitive to the photon statistics of incident waves and this feature can be used to probe their statistical properties. This could be realized by mixing classical and nonclassical drivings on an atom that should allow for the reconstruction of information on quantum statistics in the nonclassical mode [17]. Note that four-wave mixing of two coupled light modes was theoretically proposed for the quantum nondemolition measurement of the photon number in a selected mode performed by destructive measurement of photons in another coupled mode [18,19].

Here, we theoretically consider wave mixing in the case of a nonclassical photon field. We address a dynamics of a single qubit irradiated simultaneously by the coherent wave and nonclassical light. We consider two examples of a nonclassical field that is produced either by a degenerate parametric amplifier [10,20] or by a single-photon source [21–23]. We indeed find that the peaks' structure is not identical to the case of wave mixing of two continuous coherent waves—for example, some peaks turn out to be absent. For the case of a single-photon source, we get the three-peaked spectrum, which is similar to what was observed for the case of classical driving trains of pulses with relative time delay [15]. For the squeezed vacuum in one mode and a classical drive in another mode, we get only peaks containing an even number of photons from the squeezed mode, while other peaks are absent. We conclude that the peak amplitudes can be used to probe the statistical properties of incident waves.

The paper is organized as follows. In Sec. II, we consider the wave mixing under the irradiation by two coherent waves along the ideas of Ref. [17]. In Sec. III, we analyze similar equations of motion for qubit degrees of freedom under the irradiation by coherent wave and broadband squeezed light. In Sec. IV, we consider wave mixing under the irradiation by

the coherent wave and a periodically excited superposition of Fock states with 0 and 1 photons. We conclude in Sec. V.

II. WAVE MIXING UNDER THE IRRADIATION BY TWO COHERENT WAVES

Let us reproduce the main theoretical results of Ref. [17]. We consider the dynamics of the qubit coupled to the transmission line under the classical drive with two frequencies ω_1 and ω_2 close to the qubit transition frequency ω_{01}, with the amplitudes of the drives being Ω_1 and Ω_2, respectively. The relaxation of the atom Γ is radiative due to the photon emission into the waveguide and the difference between ω_1 and ω_2 is much smaller than Γ, $|\omega_1 - \omega_2| \ll \Gamma$.

We switch to the rotating frame characterized by the frequency $\omega_d = (\omega_1 + \omega_2)/2$ and introduce notations $\delta\omega = \omega_1 - \omega_d = \omega_d - \omega_2$. Maxwell-Bloch equations in this frame and under the rotating wave approximation read as

$$\frac{d\langle\sigma_-\rangle}{dt} = \langle\sigma_-\rangle(-i\Delta\omega - \gamma) - \frac{i\Omega_1}{2}e^{-i\delta\omega t}\langle\sigma_z\rangle - \frac{i\Omega_2}{2}e^{i\delta\omega t}\langle\sigma_z\rangle, \tag{1}$$

$$\frac{d\langle\sigma_z\rangle}{dt} = -\Gamma(\langle\sigma_z\rangle + 1) + i\Omega_1\left(\langle\sigma_+\rangle e^{-i\delta\omega t} - \langle\sigma_-\rangle e^{i\delta\omega t}\right) + i\Omega_2\left(\langle\sigma_+\rangle e^{i\delta\omega t} - \langle\sigma_-\rangle e^{-i\delta\omega t}\right), \tag{2}$$

where $\Delta\omega = \omega_{01} - \omega_d$, and Γ is the radiative decay rate due to the coupling to the waveguide, while γ is a decoherence rate, which also depends on the pure dephasing rate Γ_φ: $\gamma = \Gamma/2 + \Gamma_\varphi$.

It is straightforward to find a stationary solution taking into account that $\delta\omega t$ is a slowly varying phase on the timescale of Γ^{-1}. This solution can be represented as

$$\langle\sigma_z\rangle = -\left(1 + \frac{\gamma}{\Gamma}\frac{\Omega_1^2 + \Omega_2^2 + \Omega_1\Omega_2(e^{-2i\delta\omega t} + e^{2i\delta\omega t})}{(\Delta\omega)^2 + \gamma^2}\right)^{-1}, \tag{3}$$

$$\langle\sigma_-\rangle = \frac{1}{2}\frac{\Omega_1 e^{-i\delta\omega t} + \Omega_2 e^{i\delta\omega t}}{\Delta\omega - i\gamma} \times \left(1 + \frac{\gamma}{\Gamma}\frac{\Omega_1^2 + \Omega_2^2 + \Omega_1\Omega_2(e^{-2i\delta\omega t} + e^{2i\delta\omega t})}{(\Delta\omega)^2 + \gamma^2}\right)^{-1} \tag{4}$$

The amplitude of the elastically scattered wave is $-i\Gamma\langle\sigma_-\rangle/\mu$, where μ is the qubit dipole moment [17,24]. It is clear from this result that amplitudes of spectral components of the emitted power are nonzero for all frequencies divisible by $\delta\omega$ (in the rotating frame). Particularly, Eq. (4) can be rewritten as [17]

$$\langle\sigma_-\rangle = \frac{\Omega_1 e^{-i\delta\omega t} + \Omega_2 e^{i\delta\omega t}}{\Lambda}\tan\vartheta \sum_{p=-\infty}^{+\infty}[-\tan(\vartheta/2)]^{|p|}e^{i2p\delta\omega t}, \tag{5}$$

where

$$\Lambda = \frac{4\gamma\Omega_1\Omega_2}{\Gamma(\Delta\omega + i\gamma)}, \tag{6}$$

$$\vartheta = \arcsin\frac{2\gamma\Omega_1\Omega_2}{\Gamma[(\Delta\omega)^2 + \gamma^2] + \gamma(\Omega_1^2 + \Omega_2^2)}. \tag{7}$$

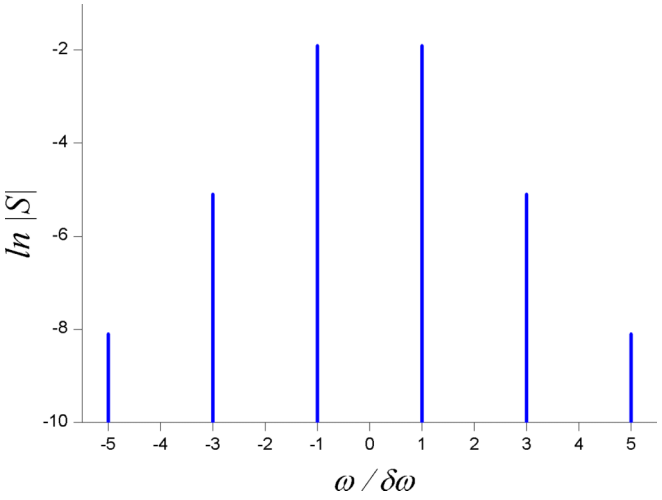

FIG. 1. Spectral components of $\langle\sigma_-\rangle$ in the case of qubit irradiation by two coherent waves (see text).

Spectral components of $\langle\sigma_-\rangle$, defined through $S(\omega) = \lim_{t\to\infty}\frac{1}{t}\int_{-t/2}^{t/2}\langle\sigma_-\rangle\exp(-i\omega t)dt$, are illustrated in Fig. 1 at $\Omega_1 = \Omega_2 = 0.15\Gamma$, $\Delta\omega = 0$, $\Gamma = 2\gamma$. A quantitatively good agreement was observed between the theory and experimental results for the case of a superconducting flux qubit irradiated by two coherent fields [17].

The wave mixing can be understood in terms of multiphoton elastic scattering involving frequencies of photons from the coherent waves [2], which correspond to the arrows in Fig. 1—lengths of arrows provide frequencies, while arrow directions show either an absorption (up) or emission (down). The absorption of two photons with frequencies ω_1 and emission of a single photon with ω_2 produces the frequency $2\omega_1 - \omega_2 = \omega_d + 3\delta\omega$ since the process is elastic and accompanied by the energy conservation. In the same way, the absorption of two photons from the ω_2 mode and emission of a single photon from ω_1 mode gives rise to the peak at $2\omega_2 - \omega_1 = \omega_d - 3\delta\omega$. These two processes correspond to the four-wave mixing. Similarly, higher-order processes involving $2l + 1$ photons are possible that result in spectral peaks at frequencies $(l + 1)\omega_1 - l\omega_2$ and $(l + 1)\omega_2 - l\omega_1$, with l being an integer number. According to the idea of Ref. [17], the intensities of the sidebands can be used to extract information about the photon statistics of incident waves.

Note that the wave mixing phenomenon is robust against energy dissipation into degrees of freedom different from photon modes. In this case, the amplitude of the elastically scattered wave is determined by a purely radiative relaxation rate, while the qubit's dynamics is described by Maxwell-Bloch equations with full Γ and γ, which incorporate losses.

For optics in the visible range, the single artificial atom is to be replaced with a cloud of identical natural atoms to achieve a strong coupling with the propagating field. In this system, there is a strong resonant absorption, so the only experimentally available configuration of bichromatic classical drive implies that $\delta\omega \gg \Gamma$. For this case, the solution for the elastic and inelastic spectrum was analytically and numerically elaborated in several works [25–27]. Particularly, it was predicted that the elastic side peaks do appear at combination

frequencies $\omega_{\pm(2l+1)} = \omega_d \pm (2l+1)\delta\omega$ and with intensities proportional to $J_0^2(2\Omega/\delta\omega)J_{2l+1}^2(2\Omega/\delta\omega)$, where $\Omega_1 = \Omega_2 = \Omega$, but no experiments demonstrating this dependence are known (here, J_l is the lth Bessel function of the first kind). Here we consider the opposite case of small $\delta\omega$, which is specifically appropriate for superconducting qubits as the frequency of the single microwave tone is controlled with great precision.

III. WAVE MIXING UNDER QUBIT IRRADIATION BY A COHERENT WAVE AND SQUEEZED LIGHT

In this section, we address the effect of the simultaneous irradiation of the qubit by the classical coherent drive with frequency ω_1 and squeezed light. As the squeezed vacuum is significantly nonclassical and has nontrivial photon statistics [28], the mixing of classical and squeezed signals will result in side components which are different from those for classical drives [17]. Thereby, wave mixing will allow one to investigate photon statistics in the nonclassical mode.

A paradigmatic example of a source of nonclassical light is the degenerate parametric amplifier described by the Hamiltonian of the driven cavity [20],

$$H_s = \omega_2 a_0^\dagger a_0 + \frac{i}{2}\left(a_0^{\dagger 2}\epsilon_s e^{-2i\omega_2 t} - a_0^2\epsilon_s^* e^{2i\omega_2 t}\right), \tag{8}$$

where a_0 is the destruction operator for the internal cavity mode with frequency ω_2, while a classical pump frequency is also ω_2. The output field of the degenerate parametric amplifier is a finite-bandwidth squeezed light. In the squeezed white-noise limit, the correlation functions of the output field can be represented as [20]

$$\langle a_{\rm out}^\dagger(t)a_{\rm out}(t')\rangle = Ne^{i\omega_2(t-t')}\delta(t-t'), \tag{9}$$

$$\langle a_{\rm out}(t)a_{\rm out}(t')\rangle = Me^{-i\omega_2(t+t')}\delta(t-t'), \tag{10}$$

where M is a measure of light squeezing. In general, $|M|^2 \leqslant N(N+1)$, while $|M|^2 = N(N+1)$ corresponds to the pure squeezed state.

The output field from the parametric amplifier is treated as an input field for the qubit [20]. The interaction between the qubit and the light is described by a usual electric-dipole approximation: $\sum_\omega g_k(a_k^\dagger\sigma_- + a_k\sigma_+)$. The equations of motion for the mean values $\langle\sigma_-\rangle$ and $\langle\sigma_z\rangle$ in the case of a qubit interacting with the output field from the degenerate parametric amplifier having central frequency close to ω_{01} are generally known from the literature [20,29–31]. They take a simple form [20] in the white-noise limit, when the bandwidth of the squeezed light significantly exceeds γ. We take into consideration the additional classical drive at another frequency ω_1 that is also close to ω_{01}, as described by the Hamiltonian $f_q(t)\sigma_x$, where $f_q(t) = -\Omega_1(e^{i\omega_1 t} + e^{-i\omega_1 t})/2$. The equations of motion in the white-noise limit (see, e.g., Eq. (10.3.2) of Ref. [20]) read as

$$\frac{d\langle\sigma_-\rangle}{dt} = \langle\sigma_-\rangle[-i\omega_{01} - \gamma(1+2N)] - \frac{i\Omega_1}{2}e^{-i\omega_1 t}\langle\sigma_z\rangle - 2\gamma Me^{-2i\omega_2 t}\langle\sigma_+\rangle, \tag{11}$$

$$\frac{d\langle\sigma_z\rangle}{dt} = -\Gamma(\langle\sigma_z\rangle + 1) - 2N\Gamma\langle\sigma_z\rangle + i\Omega_1\left(\langle\sigma_+\rangle e^{-i\omega_1 t} - \langle\sigma_-\rangle e^{i\omega_1 t}\right). \tag{12}$$

Note that the last term in the right-hand side of Eq. (11) describes a process of absorption of a photon pair accompanied by the qubit excitation. We again switch to the rotating frame characterized by the frequency $\omega_d = (\omega_1+\omega_2)/2$ as in the case of two coherent fields. The stationary solution in the rotating wave approximation is

$$\langle\sigma_z\rangle = -\frac{1}{1+2N} + \frac{\gamma\Omega_1^2}{\Gamma(1+2N)}\frac{1 + \frac{M}{2N+1}e^{4i\delta\omega t} + \frac{M^*}{2N+1}e^{-4i\delta\omega t}}{(\Delta\omega)^2 + \gamma^2[(2N+1)^2 - 4|M|^2] + \frac{\gamma\Omega_1^2}{\Gamma}\left(1 + \frac{M}{2N+1}e^{4i\delta\omega t} + \frac{M^*}{2N+1}e^{-4i\delta\omega t}\right)}, \tag{13}$$

$$\langle\sigma_-\rangle = \frac{\Omega_1}{2}\frac{(i\gamma + \frac{\Delta\omega}{2N+1})e^{-i\delta\omega t} + i\gamma\frac{2M}{2N+1}e^{3i\delta\omega t}}{(\Delta\omega)^2 + \gamma^2[(2N+1)^2 - 4|M|^2] + \frac{\gamma\Omega_1^2}{\Gamma}\left(1 + \frac{M}{2N+1}e^{4i\delta\omega t} + \frac{M^*}{2N+1}e^{-4i\delta\omega t}\right)}. \tag{14}$$

We see from Eq. (14) that

(i) the peaks structure in the spectrum is not identical to the similar structure in the case of two coherent fields,

(ii) nonzero squeezing M together with a classical drive produces side peaks, and

(iii) without a classical drive, no peak appears under the irradiation by only a squeezed light.

Spectral components $S(\omega)$ of $\langle\sigma_-\rangle$ are shown in Fig. 2 at $\Omega_1 = 0.15\Gamma$, $\Delta\omega = 0$, and $\Gamma = 2\gamma$ and for the pure squeezed state with $2|M|/(2N+1) \simeq 1$, where M is real. Compared to Fig 1, the spectrum is shifted and some peaks are absent.

The obtained results can be qualitatively explained as follows. In the absence of a coherent drive, the photon field at the qubit is just a broadband output field from the degenerate parametric amplifier which contains correlated photon pairs [20], with each pair having total energy $2\omega_2$. This means that there is no resonant frequency for a single photon since the radiated field is broadband, but there is such a frequency for each correlated photon pair. Therefore, no peak appears in the spectrum of $\langle\sigma_-\rangle$ without an additional coherent field. For the same reason, there is no peak at $\delta\omega$ also in the presence of this field.

The first side peak appears at $3\delta\omega$ and it corresponds to the multiphoton process when a photon *couple* with total frequency $2\omega_2$ is absorbed and a single photon with the frequency ω_1 is emitted, giving rise to the output photon with $2\omega_2 - \omega_1 = \omega_d - 3\delta\omega$. This process is illustrated in Fig. 3(a). The dominant contribution to the amplitude is proportional to both Ω_1/Γ and M, since M provides a number of correlated photon pairs in the incident nonclassical light. The peak at

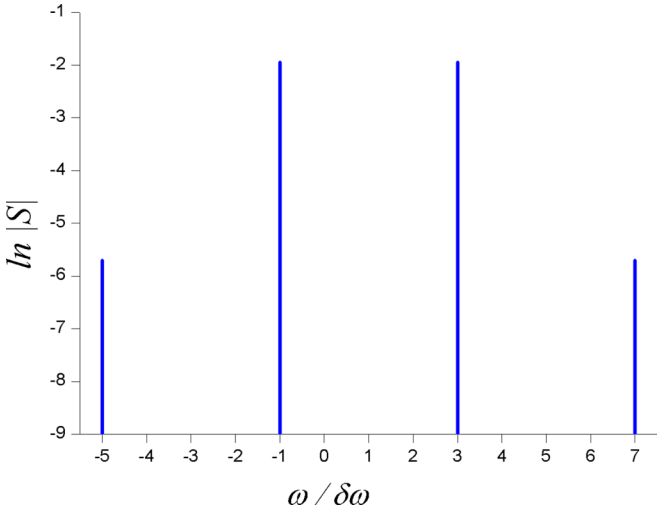

FIG. 2. Spectral components of $\langle\sigma_-\rangle$ in the case of qubit irradiation by a coherent wave together with the pure squeezed light (see text).

$-5\delta\omega$ appears as a result of the absorption of three photons of frequency ω_1 and the emission of a photon couple having a total frequency $2\omega_2$; this mechanism produces output photons with frequency $3\omega_1 - 2\omega_2 = \omega_d + 5\delta\omega$; see Fig. 3(b). The amplitude is proportional to the product of M^* and $(\Omega_1/\Gamma)^3$. The peak at $7\delta\omega$ appears as a result of the absorption of two pairs with $2\omega_2$ and the emission of three photons with ω_1; the amplitude is therefore proportional to the product of M^2 and $(\Omega_1/\Gamma)^3$ since two correlated photon pairs are involved [see Fig. 3(c)], and so on.

In the weak driving regime, $\Omega_1 \ll \Gamma$, and at the resonance, $\Delta\omega = 0$, Eq. (14) can be represented as

$$\langle\sigma_-\rangle \approx \frac{if\Gamma}{\Omega_1}\left(fe^{-i\delta\omega t} + fme^{3i\delta\omega t} - f^3m^*e^{-5i\delta\omega t} - f^3m^2e^{7i\delta\omega t} + \cdots\right), \tag{15}$$

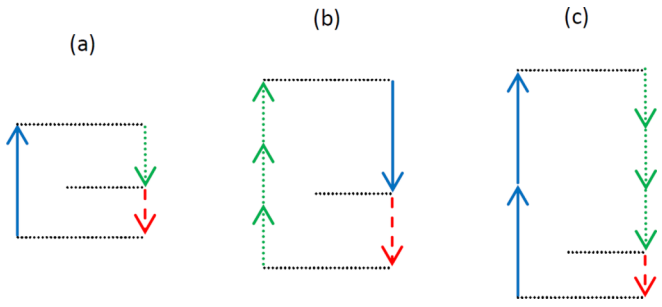

FIG. 3. Schematic images of multiphoton processes resulting in different side peaks in the emission spectra at (a) $3\delta\omega$, (b) $-5\delta\omega$, and (c) $7\delta\omega$. Blue arrows (solid lines) show the absorption and emission of correlated photon pairs with total energy $2\omega_2$. Green arrows (dotted lines) correspond to single photons with energies ω_1. Red arrows (dashed lines) indicate photon emission, which is responsible for the side peaks.

where, for simplicity, we assumed that pure dephasing is negligible, so that $\gamma = 2\Gamma$,

$$f = \frac{\Omega_1}{\sqrt{2\Gamma\gamma[(2N+1)^2 - 4|M|^2]}}, \tag{16}$$

$$m = \frac{2M}{2N+1}. \tag{17}$$

We see that apart from the general prefactor, $\langle\sigma_-\rangle$ in the stationary state is a sum of contributions, which correspond to different multiphoton processes, with each contribution being proportional to f in a power given by the number of photons in the coherent wave participating in this process, as well as to the squeezing characteristics m, which depend on the total number of correlated pairs in the nonclassical wave, in a power given by the number of correlated photon pairs also participating in a given process. The side peaks at $\delta\omega(1+4l)$, where l is an arbitrary integer number, are absent since there is no multiphoton process that can produce these peaks. The obtained results also evidence that the squeezing parameter can be reconstructed from the analysis of the side peaks' amplitudes in the emission spectra—for example, a direct comparison of the two largest peak amplitudes at $-\delta\omega$ and $3\delta\omega$ directly gives m.

IV. WAVE MIXING UNDER QUBIT IRRADIATION BY A COHERENT WAVE AND QUANTUM SUPERPOSITION OF VACUUM AND ONE PHOTON

In this section, we consider another example of wave mixing, when nonclassical light is represented by periodically generated superpositions of Fock states with 0 and 1 photons. We assume that the additional qubit serves as a emitter and creates the mentioned superpositions in the semi-infinite waveguide due to strong coupling with the continuum of modes. This source for quantum superpositions of vacuum and one photon can be engineered, for example, on the basis of the ideas of Refs. [21,22], where tunable single-photon sources constructed from artificial superconducting atoms were demonstrated. The emitter is periodically excited by a strong external drive, which brings it to a quantum mechanical superposition of the lowest-energy state $|\downarrow\rangle$ and excited state $|\uparrow\rangle$ with fixed weights. The relaxation of the excited state is radiative due to the single-photon emission into the line. Let us denote a tunable probability for the photon to be emitted after the excitation pulse as ν. The excitation pulse is assumed to be much shorter than the emitter relaxation characteristic time $1/\gamma_e$. Hereafter, indices e are referred to as the emitter. The time interval between two excitation pulses T is much larger than $1/\gamma_e$. Using a Bloch sphere representation, the emitter state at $t = Tn$, with n being an integer number, can be expressed as

$$\langle\sigma_-^e(Tn)\rangle = \frac{\sin\theta}{2}e^{-i\omega_{01}^e Tn}, \tag{18}$$

$$\left\langle\sigma_z^e(Tn)\right\rangle = \cos\theta, \tag{19}$$

where θ is a polar angle, $\cos\theta = 2\nu - 1$. Equivalently, the same state can be represented as $\sqrt{1-\nu}\,|\downarrow\rangle + e^{-i\omega_{01}^e Tn}\sqrt{\nu}\,|\uparrow\rangle$. The presence of the phase factor $e^{-i\omega_{01}^e Tn}$ implies that the emitter is excited by the Rabi pulse, with

the frequency ω_{01}^e coinciding with the emitter transition frequency. The excitation is assumed not to alter the quantum state of the second qubit, which is responsible for the wave mixing, that can be achieved in experiments by using different methods. The emitter relaxation creates the superposition of 0 and 1 photons in the waveguide. These photon states are then mixed with the continuous classical monochromatic drive of frequency ω_1 and amplitude Ω_1 when they together irradiate the second qubit characterized by the dissipation rate $\gamma \sim \gamma_e$. Since the nonclassical signal at the second qubit's position at any time instance contains no more than a single photon ($T \gg 1/\gamma$), the side peaks' structure must be distinct from the case of wave mixing under two coherent drives because higher-order mixing processes cannot take place.

The presence of the qubit emitter can be described by an interaction term [30], which has a form $\sqrt{\gamma\gamma_e}(\sigma_+\sigma_-^e + \sigma_-\sigma_+^e)$. It corresponds to the interaction of two qubits via a photon field treated in the Markov approximation and can be derived using, e.g., a chain of equations of motion in the Heisenberg picture. Since much less attention has been paid in the literature for such a problem of qubit dynamics under the irradiation from the quantum emitter, we include a microscopic derivation of the equations of motion in Appendix. This derivation is based on the Heisenberg equations of motion. The modification of the Maxwell-Bloch equations now takes the form

$$\frac{d\langle\sigma_-\rangle}{dt} = \langle\sigma_-\rangle(-i\omega_{01} - \gamma) - \frac{i\Omega_1}{2}e^{-i\omega_1 t}\langle\sigma_z\rangle + \sqrt{\gamma\gamma_e}\langle\sigma_z\sigma_-^e\rangle, \tag{20}$$

$$\frac{d\langle\sigma_z\rangle}{dt} = -\Gamma(\langle\sigma_z\rangle + 1) + i\Omega_1\left(\langle\sigma_+\rangle e^{-i\omega_1 t} - \langle\sigma_-\rangle e^{i\omega_1 t}\right) + 2\sqrt{\gamma\gamma_e}(\langle\sigma_-\sigma_+^e\rangle + \langle\sigma_+\sigma_-^e\rangle). \tag{21}$$

The right-hand sides of both equations contain correlators $\langle\sigma_z\sigma_-^e\rangle$, $\langle\sigma_-\sigma_+^e\rangle$, and $\langle\sigma_+\sigma_-^e\rangle$, which cannot be factorized due to the fact that we consider an ultraquantum limit and this fact makes the situation distinct from the case of qubit irradiation by classical signals. We treat these correlators as follows. We first consider a steady state of the qubit under the irradiation of only a classical drive and at $t = Tn$,

$$\langle\sigma_z(Tn)\rangle = -\left(1 + \frac{\gamma}{\Gamma}\frac{\Omega_1^2}{(\Delta\omega)^2 + \gamma^2}\right)^{-1}, \tag{22}$$

$$\langle\sigma_-(Tn)\rangle = \frac{1}{2}\frac{\Omega_1 e^{-i\omega_1 Tn}}{\Delta\omega - i\gamma}\left(1 + \frac{\gamma}{\Gamma}\frac{\Omega_1^2}{(\Delta\omega)^2 + \gamma^2}\right)^{-1}. \tag{23}$$

Note that these two equations can be obtained from Eqs. (3) and (4) by assuming that the amplitude of one of the classical signals is zero, $\Omega_2 = 0$. Now we obtain, from Eqs. (18), (19), (22), and (23),

$$\langle\sigma_z\sigma_-^e(Tn)\rangle = \langle\sigma_z(Tn)\rangle\langle\sigma_-^e(Tn)\rangle = -\left(1 + \frac{\gamma}{\Gamma}\frac{\Omega_1^2}{(\Delta\omega)^2 + \gamma^2}\right)^{-1}\frac{\sin\theta}{2}e^{-i\omega_{01}^e Tn}, \tag{24}$$

$$\langle\sigma_-\sigma_+^e(Tn)\rangle = \langle\sigma_-(Tn)\rangle\langle\sigma_+^e(Tn)\rangle = \frac{1}{2}\frac{\Omega_1}{\Delta\omega - i\gamma}\left(1 + \frac{\gamma}{\Gamma}\frac{\Omega_1^2}{(\Delta\omega)^2 + \gamma^2}\right)^{-1} \times \frac{\sin\theta}{2}e^{i(\omega_{01}^e - \omega_1)Tn}. \tag{25}$$

The equations of motion for these correlators at $t \in (Tn, Tn + T)$ read as

$$\frac{d\langle\sigma_z\sigma_-^e\rangle}{dt} = \langle\sigma_z\sigma_-^e\rangle(-i\omega_{01}^e - \Gamma - \gamma_e), \tag{26}$$

$$\frac{d\langle\sigma_-\sigma_+^e\rangle}{dt} = \langle\sigma_-\sigma_+^e\rangle\left(i\left(\omega_{01}^e - \omega_{01}\right) - \gamma - \gamma_e\right). \tag{27}$$

From these two equations, we obtain

$$\langle\sigma_z\sigma_-^e(t)\rangle = -|\langle\sigma_z\sigma_-^e(Tn)\rangle|e^{-i\omega_{01}^e Tn}e^{-i\omega_{01}^e(t-Tn)}e^{-(\Gamma+\gamma_e)(t-Tn)}, \tag{28}$$

$$\langle\sigma_-\sigma_+^e(t)\rangle = |\langle\sigma_-\sigma_+^e(Tn)\rangle|e^{i(\omega_{01}^e - \omega_1)Tn} \times e^{i(\omega_{01}^e - \omega_{01})(t-Tn)}e^{-(\gamma+\gamma_e)(t-Tn)}. \tag{29}$$

Note that in principle, the dynamics of the correlators $\langle\sigma_z\sigma_-^e\rangle$, $\langle\sigma_-\sigma_+^e\rangle$, and $\langle\sigma_+\sigma_-^e\rangle$ is determined by full equations of motions for these quantities, which, for instance, also include an external drive of frequency ω_1. However, it can be shown that the simplified equations of motion (26) and (27) produce correct results, while omitted terms give only small additive contributions, which do not alter the general conclusions on the spectrum structure.

The quantities (28) and (29) can be used as inputs for Eqs. (20) and (21)—they provide additional nonclassical driving of the qubit. We also take into account that ω_{01}^e can be associated with the frequency of the drive ω_2: $\omega_2 \equiv \omega_{01}^e$. We then switch to the rotating frame characterized by the frequency ω_d and use the same notations as in Sec. II. We also extend t from $t \in (Tn, Tn + T)$ to $t \in (-\infty, +\infty)$. This means that $(t - Tn)$ in Eqs. (20) and (21) must be replaced by $\lfloor t/T \rfloor T$, where $\lfloor \ldots \rfloor$ is a floor function. The equations of motion take the form

$$\frac{d\langle\sigma_-\rangle}{dt} = \langle\sigma_-\rangle(-i\Delta\omega - \gamma) - \frac{i\Omega_1}{2}e^{-i\delta\omega t}\langle\sigma_z\rangle + \sqrt{\gamma\gamma_e}|\langle\sigma_z\sigma_-^e(Tn)\rangle|e^{i\delta\omega t}e^{-(\Gamma+\gamma_e)\lfloor t/T\rfloor T}, \tag{30}$$

$$\frac{d\langle\sigma_z\rangle}{dt} = -\Gamma(\langle\sigma_z\rangle + 1) + i\Omega_1\left(\langle\sigma_+\rangle e^{-i\delta\omega t} - \langle\sigma_-\rangle e^{i\delta\omega t}\right) + 2\sqrt{\gamma\gamma_e}|\langle\sigma_-\sigma_+^e(Tn)\rangle| \times \left(e^{-2i\delta\omega t}e^{i(\delta\omega - \Delta\omega)\lfloor t/T\rfloor T} + \text{c.c.}\right)e^{-(\gamma+\gamma_e)\lfloor t/T\rfloor T}. \tag{31}$$

We treat these equations as follows. Within each time interval $t \in (Tn, Tn + T)$, functions of the form $e^{-(\gamma+\gamma_e)\lfloor t/T\rfloor T}$ are approximated as 1 at $t - Tn \lesssim \gamma^{-1}, \gamma_e^{-1}$ and 0 otherwise (steplike irradiation by the nonclassical signal). For the first interval of time, it is readily seen from the above equations that $\langle\sigma_-\rangle$ is a superposition of three contributions proportional to $e^{i\delta\omega t}$, $e^{-i\delta\omega t}$, and $e^{-3i\delta\omega t}$, while $\langle\sigma_z\rangle$ is a superposition of terms of the form $e^{2i\delta\omega t}$ and $e^{-2i\delta\omega t}$. For the second time

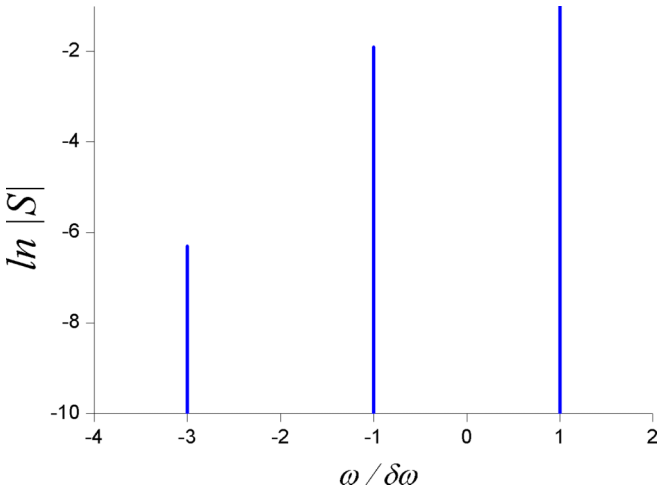

FIG. 4. Spectral components of $\langle\sigma_-\rangle$ in the case of qubit irradiation by a coherent wave together with the superposition of Fock states with 0 and 1 photon (see text).

interval, when only a classical drive acts on the qubit, $\langle\sigma_-\rangle$ contains only a contribution of the form $e^{-i\delta\omega t}$. Thus, at low frequencies $\omega \ll \gamma^{-1}$, there appear only three spectral components of $\langle\sigma_-\rangle$. This is due to the limitation of the photon number in the nonclassical signal since this situation is totally different from the previously considered setups.

An equivalent qualitative picture can be obtained by considering a stationary state solution and neglecting time derivatives in the right-hand sides of Eqs. (30) and (31). The solution can be represented as

$$\langle\sigma_-\rangle = c_1 e^{i\delta\omega t} + c_{-1} e^{-i\delta\omega t} + c_{-3} e^{-3i\delta\omega t}. \tag{32}$$

The expressions of coefficients c_1, c_{-1}, and c_{-3}, in the general case, are rather cumbersome so we present them only for $\Delta\omega = 0$ and in leading order in Ω_1/Γ,

$$c_1 \simeq -\sqrt{\frac{\gamma_e}{\gamma}}\frac{\sin\theta}{2}, \tag{33}$$

$$c_{-1} \simeq \frac{i\Omega_1}{2\gamma}, \tag{34}$$

$$c_{-3} \simeq \frac{\Omega_1^2}{2\gamma^2}\frac{\sqrt{\gamma\gamma_e}}{\Gamma}\frac{\sin\theta}{2} \times \left(e^{-(\gamma+\gamma_e)\lfloor t/T\rfloor T} e^{i\delta\omega\lfloor t/T\rfloor T} + e^{-(\Gamma+\gamma_e)\lfloor t/T\rfloor T}\right). \tag{35}$$

Thus, at low frequencies $\omega \ll \gamma^{-1}$, there appear only three spectral components of $\langle\sigma_-\rangle$. They are shown in Fig. 4 at $\Omega_1 = 0.15\Gamma$, $\Delta\omega = 0$, $\Gamma = 2\gamma$, $\gamma = \gamma_e$, $\nu = 1/2$, and $T = 5/\gamma_e$. The only side component is given by the third term in the right-hand side of Eq. (32). It appears due to the absorption of two photons of the coherent wave with frequency ω_1 and the emission of a single photon at frequency ω_2 since there can be no more than a single photon in the second signal which is fundamentally nonclassical. This process is illustrated in Fig. 5. The spectrum therefore is totally different from the spectrum in the case of two coherent waves mixing, which was described in Sec. II; see Fig. 1. Note that c_{-3} is proportional to $(\Omega_1/\Gamma)^2$, which is consistent with the fact that two photons from the coherent wave are mixed with zero or one photon of

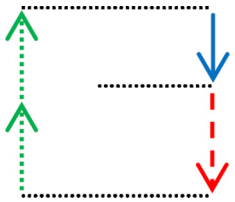

FIG. 5. Schematic image of a multiphoton process resulting in a side peak in the emission spectra at $3\delta\omega$ under the qubit irradiation by the classical signal and quantum superpositions of Fock states with 0 and 1 photons. Green arrows (dotted lines) correspond to photons from the coherent wave with energies ω_1. Blue arrow (solid line) corresponds to the single photon with energy ω_2. Red arrow (dashed line) indicates photon emission with energy $2\omega_1 - \omega_2 = \omega_d + 3\delta\omega$.

the nonclassical field within each time "window" T. Another interesting observation is that the effect of the nonclassical signal is strongest at $\nu = 1/2$ and not at $\nu = 1$. This is due to the fact that the single-photon Fock state contains no information about the phase.

V. CONCLUSIONS

To conclude, we considered theoretically wave mixing between the classical monochromatic signal and a nonclassical light. The mixing occurs due to the interaction of two photon fields on a single qubit that gives rise to elastic multiphoton processes. Two particular examples of nonclassical light were addressed: broadband squeezed light that can be produced by the degenerate parametric amplifier and a periodically excited superposition of Fock states with 0 and 1 photons that can be generated by a single-photon source.

The spectrum for the emitted light, which contains side peaks attributed to nonlinearities of various orders, is distinct from the similar spectrum in the case of qubit irradiation by two classical drives. The reason is that nonclassical photon fields are characterized by zero occupancies of certain Fock states. For example, in the case of a finite-bandwidth squeezed light, only multiphoton processes involving correlated pairs of the squeezed field contribute to the side peaks' amplitudes. Such a restriction is even more strict for Fock states with 0 and 1 photons, so that only a single side peak appears in this case.

Thus, the amplitudes of side peaks can be used to probe nonclassical light statistics. The key idea is that light, whose statistical properties have to be determined, must be mixed with the classical signal on a single artificial atom. The absence of some peaks in the elastic spectrum of the emitted light compared to the case of mixing of two classical signals shows that the first signal is strongly nonclassical since occupancies of certain Fock states must be zero for these peaks to be absent.

ACKNOWLEDGMENTS

We thank A. M. Satanin, A. A. Elistratov, E. S. Andrianov, O. V. Kotov, and D. S. Shapiro for very useful discussions. W.V.P. acknowledges support from RFBR (Project No. 19-02-00421). A.Yu.D. and O.V.A. acknowledge support from Russian Science Foundation, Grant No. 21-72-30026.

APPENDIX: QUBIT IRRADIATION BY A COHERENT WAVE AND QUANTUM SUPERPOSITION OF VACUUM AND ONE PHOTON: EQUATIONS OF MOTION

1. Hamiltonian and preliminaries

We consider a single qubit coupled to the waveguide, which experiences the simultaneous effect of a classical monochromatic drive and irradiation from the source of $0+1$ states, which is represented by another qubit (emitter). The equations of motion are derived from the microscopic theory.

We assume that the one-dimensional space is discrete and the distance between nearest points is δ, while the number of points is $N_s \to \infty$. The discreteness will be eliminated at the end from all observables; this is a technical issue. The creation and destruction operators $a_R^\dagger$ and a_R for photons in a given point R are constructed from delocalized states described by $a_k^\dagger$ and a_k as

$$a_R^\dagger = \frac{1}{\sqrt{N_s}} \sum_k \exp(-ikr) a_k^\dagger. \tag{A1}$$

Here, k is allowed to take the form $-\frac{\pi}{\delta} + \frac{2\pi m}{L}$, where integer m ranges from 0 to $N_s - 1$, while $L = N_s\delta$ is the system's length. Thus, the maximum ω_k is $\omega_{\max} = \pi c/\delta$. The difference between two closest values of energy is $2\pi c/L$, so that the density of energy states is $\rho = L/2\pi c$.

The Hamiltonian of the whole system can be represented as

$$H = H_{\text{phot}} + H_q + H_{\text{int}} + H_e + H_{\text{int}}^{(e)}, \tag{A2}$$

where

$$H_{\text{phot}} = \sum_k \omega_k a_k^\dagger a_k \tag{A3}$$

is a photon Hamiltonian. The second term H_q is the Hamiltonian of the qubit under the classical drive,

$$H_q = \frac{\omega_{01}}{2}\sigma_z - f_q(t)(\sigma_+ + \sigma_-). \tag{A4}$$

The third term H_{int} represents an interaction between the qubit placed at r and the photon field,

$$H_{\text{int}} = \frac{1}{\sqrt{N_s}} \sum_k (e^{-ikr} g_k^* a_k^\dagger \sigma_- + e^{ikr} g_k a_k \sigma_+), \tag{A5}$$

where r is qubit coordinate and g_k is an interaction constant defined as

$$g_k = -i\sqrt{\frac{\omega_k}{2\epsilon_0 \delta}}\mu. \tag{A6}$$

The fourth term H_e is the emitter Hamiltonian,

$$H_e = \frac{\omega_{01}^{(e)}}{2}\sigma_z^{(e)}. \tag{A7}$$

The fifth term $H_{\text{int}}^{(e)}$ describes the interaction between the emitter positioned at r_e and photon field,

$$H_{\text{int}}^{(e)} = \frac{1}{\sqrt{N_s}} \sum_k (e^{-ikr_e} g_k^{(e)*} a_k^\dagger \sigma_-^{(e)} + e^{ikr_e} g_k^{(e)} a_k \sigma_+^{(e)}), \tag{A8}$$

where r_e is the emitter coordinate, and $g_k^{(e)}$ is defined in a similar way as g_k. The term (A8) is responsible for periodical excitation of the $|0\rangle + |1\rangle$ states through the emitter relaxation. We do not explicitly take into consideration an external drive which excites the emitter. Notice that we also use a slightly nonstandard definition of the interaction constant since we extracted $1/\sqrt{N_s}$ from it to the prefactor in Eqs. (A5) and (A8). The prefactor is usually absorbed by g_k, and the latter then scales as $1/\sqrt{L}$. We stress that finally, the interaction constant will be expressed via the qubit relaxation rate.

If the dependence of g_k on ω_k can be neglected, the interaction is determined by the local photon field a_r at the position of the qubit, as can be verified by performing a summation in Eq. (A5),

$$H_{\text{int}} \sim (a_r^\dagger \sigma_- + a_r \sigma_+). \tag{A9}$$

2. Equations of motion

We are going to explore the dynamics of the system and focus on the steady state. There is no need to phenomenologically introduce any energy dissipation associated with the qubit within our treatment since dissipation is due to the decay of the qubit excited state into the continuum of photon modes. These modes as well as their interaction with the qubit are included in the Hamiltonian.

Let us consider an infinite chain of equations of motion for the qubit in the Heisenberg picture. The equations of motion for $\langle\sigma_-\rangle$ and σ_z read as

$$\frac{d\langle\sigma_-\rangle}{dt} = -i\omega_{01}\langle\sigma_-\rangle - if_q\langle\sigma_z\rangle + \frac{i}{\sqrt{N_s}} \sum_k e^{ikr} g_k \langle a_k \sigma_z\rangle, \tag{A10}$$

$$\frac{d\langle\sigma_z\rangle}{dt} = 2if_q(\langle\sigma_+\rangle - \langle\sigma_-\rangle) + \frac{2i}{\sqrt{N_s}} \sum_k (e^{-ikr} g_k^* \langle a_k^\dagger \sigma_-\rangle - e^{ikr} g_k \langle a_k \sigma_+\rangle). \tag{A11}$$

They depend on higher-order correlators. The equations of motion for them are

$$\frac{d\langle a_k\sigma_z\rangle}{dt} = -i\omega_k\langle a_k\sigma_z\rangle - 2if_q(\langle a_k\sigma_-\rangle - \langle a_k\sigma_+\rangle) + \frac{2i}{\sqrt{N_s}}\sum_p (e^{-ipr}g_p^*\langle a_p^\dagger a_k\sigma_-\rangle - e^{ipr}g_p\langle a_p a_k\sigma_+\rangle)$$
$$+ \frac{i}{\sqrt{N_s}}e^{-ikr}g_k^*\langle\sigma_-\rangle + \frac{i}{\sqrt{N_s}}e^{-ikr_e}g_k^{e*}\langle\sigma_-^e\sigma_z\rangle, \tag{A12}$$

$$\frac{d\langle a_k\sigma_+\rangle}{dt} = i(\omega_{01}-\omega_k)\langle a_k\sigma_+\rangle + if_q\langle a_k\sigma_z\rangle - \frac{i}{\sqrt{N_s}}\sum_p e^{-ipr}g_p^*\langle a_p^\dagger a_k\sigma_z\rangle - \frac{i}{2\sqrt{N_s}}e^{-ikr}g_k^*(\langle\sigma_z\rangle + 1)$$
$$- \frac{i}{\sqrt{N_s}}e^{-ikr_e}g_k^{e*}\langle\sigma_-^{(e)}\sigma_+\rangle, \tag{A13}$$

which depend on next-order correlators, and so on.

Note that in most of the situations, the dependence of g_k on ω_k can be neglected, and therefore the correlators from the right-hand side (RHS) of the above equations are reduced to the correlators involving the local photon field strictly at the qubit position (after the summations over p).

The infinite chain of equations of motion is untractable. Therefore, certain approximations must be made. In general, our system must be well described by the Born-Markov approximation. It assumes that there is no back action of the field emitted by the qubit on qubit. We limit ourselves to the second order in g, which means that we adopt the Born approximation. In this case, we can truncate the infinite chain of equations and consider only the system (A10)–(A13). We can also neglect $\langle a_k\sigma_-\rangle$ in the right-hand side of Eq. (A12) that is justified in the rotating-wave approximation.

Let us now concentrate on Eqs. (A12) and (A13). A simplification comes from the fact that terms proportional to f_q can be omitted in the right-hand sides of these two equations since they produce corrections of the order of Ω_1/Ω_{01}. This approximation will allow us to decouple Eqs. (A12) and (A13). We also split the correlators as $\langle a_p^\dagger a_k\sigma_-\rangle \simeq \langle a_p^\dagger a_k\rangle\langle\sigma_-\rangle$, $\langle a_p^\dagger a_k\sigma_z\rangle \simeq \langle a_p^\dagger a_k\rangle\langle\sigma_z\rangle$, and $\langle a_p a_k\sigma_+\rangle \simeq \langle a_p a_k\rangle\langle\sigma_+\rangle$, which is justified in the Born approximation. This implies that these two quantities generated by the emitter will be treated as inputs for the qubit's dynamics.

Now we address a couple of equations, which are Eqs. (A10) and (A12). The solution of Eq. (A12) can be formally written in the integral form as

$$\langle a_k(t)\sigma_z(t)\rangle = \frac{i}{\sqrt{N_s}}\int_0^t dt' e^{i\omega_k(t'-t)}\langle\sigma_-(t')\rangle\left(e^{-ikr}g_k^* + 2\sum_p e^{-ipr}g_p^*\langle a_p^\dagger(t')a_k(t')\rangle\right)$$
$$+ \frac{i}{\sqrt{N_s}}e^{-ikr_e}g_k^{e*}\int_0^t dt' e^{i\omega_k(t'-t)}\langle\sigma_-^e(t')\sigma_z(t')\rangle. \tag{A14}$$

We neglected the correlator of the form a^2 in the RHS of the above equation since it is irrelevant for the quantum source that we consider here, provided pulses from it are well separated in time. However, it can be relevant for overlapping pulses. We now adopt the Markov approximation, which is based on the observation that there exists a separation between fast and slow variables in the integrands. Particularly, we insert $\langle\sigma_-(t')\rangle \simeq \langle\sigma_-(t)\rangle e^{i\omega_{01}(t-t')}$ into the second integral in the RHS of Eq. (A14).

Now we substitute Eq. (A14) into Eq. (A10). The first term in the RHS of Eq. (A14) provides the following contribution to the RHS of Eq. (A10):

$$-\frac{\langle\sigma_-\rangle}{N_s}\sum_k |g_k|^2\int_0^t dt' e^{i(\omega_k-\omega_{01})(t'-t)}. \tag{A15}$$

The integral in the RHS of Eq. (A15), as well as other similar integrals appearing in the derivation of the equations of motion, is evaluated as

$$\int_0^t dt' e^{i(\omega_k-\omega_{01})(t'-t)} = \int_0^t dt'[\cos(\omega_k-\omega_{01})(t'-t) + i\sin(\omega_k-\omega_{01})(t'-t)]$$
$$= \int_0^t dt'\cos(\omega_k-\omega_{01})(t'-t) + \frac{i}{\omega_k-\omega_{01}}[-1+\cos(\omega_k-\omega_{01})t], \tag{A16}$$

where the last term vanishes after averaging over long time. The first term then gives a dissipation rate since the integral is nonzero and equal to $\approx t$ only at $(\omega_k-\omega_{01})t \lesssim \pi$ and the number of energy states satisfying this condition is ρ/t. Therefore, the expression (A15) is reduced to $-N_s^{-1}\rho|g_{k_{01}}|^2\langle\sigma_-\rangle$. The combination $N_s^{-1}\rho|g_{k_{01}}|^2$ is simply the energy dissipation rate γ (in the absence of pure dephasing). It is important to stress that it turns out to be independent both on L and δ. The second term in the RHS of Eq. (A16) is responsible for the Lamb shift, $\Delta_L = N_s^{-1}\sum_k |g_k|^2(\omega_k-\omega_{01})^{-1}$. We absorb it into the definition of ω_{01} in Eq. (A10). Finally, Eq. (A10) in the Born-Markov approximation takes the form

$$\frac{d\langle\sigma_-\rangle}{dt} = -i\omega_{01}\langle\sigma_-\rangle - if_q\langle\sigma_z\rangle + \sqrt{\gamma\gamma_e}\langle\sigma_-^e\sigma_z\rangle - 2\gamma\langle\sigma_-\rangle\langle a_r^\dagger a_r\rangle - \gamma\langle\sigma_-\rangle. \tag{A17}$$

Let us consider Eqs. (A11) and (A13). The solutions of Eq. (A13) can be formally written in the integral form as

$$\langle a_k(t)\sigma_+(t)\rangle = -\frac{ig_k^* e^{-ikr}}{2\sqrt{N_s}}\int_0^t dt' e^{i(\omega_k-\omega_{01})(t'-t)}(\langle\sigma_z(t')\rangle+1)\rangle - \frac{i}{\sqrt{N_s}}\int_0^t dt' e^{i(\omega_k-\omega_{01})(t'-t)}\sum_p g_p^* e^{-ipr}\langle a_p^\dagger(t')a_k(t')\rangle - \frac{i}{\sqrt{N_s}}e^{-ikr_e}g_k^{e*}\int_0^t dt' e^{i(\omega_k-\omega_{01})(t'-t)}\langle\sigma_-^{(e)}(t')\sigma_+(t')\rangle. \tag{A18}$$

In the Markov approximation, $\langle\sigma_z(t')\rangle$ in the integrand can be replaced by $\langle\sigma_z(t)\rangle$.

We substitute Eq. (A18) into Eq. (A11) and collect all the terms. Within the Markov approximation, we obtain

$$\frac{d\langle\sigma_z\rangle}{dt} = -\Gamma(1+\langle\sigma_z\rangle) - 2\Gamma\langle\sigma_z\rangle\langle a_r^\dagger a_r\rangle + 2if_q(\langle\sigma_+\rangle - \langle\sigma_-\rangle) + 2\sqrt{\gamma\gamma_e}(\langle\sigma_+^{(e)}\sigma_-\rangle + \text{c.c.}), \tag{A19}$$

where $\Gamma = 2\gamma$ (pure dephasing has been neglected) .

Thus, Eqs. (A17) and (A19) provide a pair of the equations of motion for the qubit coupled to the emitter. Notice that in our case, $\langle a_r^\dagger a_r\rangle$ in the RHS of both equations can be omitted. Indeed, for the qubit under the mixed drive, these quantities are nonzero only within each time window of duration $\sim 1/\gamma_e$ after the emitter relaxation. The mean value $\langle a_r^\dagger a_r\rangle$ carries no information about the phase, so it does not influence our qualitative result on the structure of the spectrum. If needed, $\langle a_r^\dagger a_r\rangle$ can be found from the equations of motion for the emitter.

[1] Y. R. Shen, *The Principles of Nonlinear Optics*, 1st ed. (Wiley, New York, 1984).

[2] R. Boyd, *Nonlinear Optics*, 3rd ed. (Academic, Cambridge, MA, 2008).

[3] G. P. Agrawal, *Nonlinear Fiber Optics*, 4th ed. (Academic, Cambridge, MA,2007).

[4] A. F. van Loo, A. Fedorov, K. Lalumière, B. C. Sanders, A. Blais, and A. Wallraff, Photon-mediated interactions between distant artificial atoms, Science **342**, 1494 (2013).

[5] M. Hofheinz, H. Wang, M. Ansmann, R. C. Bialczak, E. Lucero, M. Neeley, A. D. O'Connell, D. Sank, J. Wenner, J. M. Martinis, and A. N. Cleland, Synthesizing arbitrary quantum states in a superconducting resonator, Nature (London) **459**, 546 (2009).

[6] I.-C. Hoi, A. F. Kockum, T. Palomaki, T. M. Stace, B. Fan, L. Tornberg, S. R. Sathyamoorthy, G. Johansson, P. Delsing, and C. M. Wilson, Giant Cross-Kerr Effect for Propagating Microwaves Induced by an Artificial Atom, Giant cross-Kerr Effect for Propagating Microwaves Induced by an Artificial Atom, Phys. Rev. Lett. **111**, 053601 (2013).

[7] D. Roy, C. M. Wilson, and O. Firstenberg, Colloquium: Strongly interacting photons in one-dimensional continuum, Rev. Mod. Phys. **89**, 021001 (2017).

[8] W. R. Kelly, Z. Dutton, J. Schlafer, B. Mookerji, T. A. Ohki, J. S. Kline, and D. P. Pappas, Direct Observation of Coherent Population Trapping in a Superconducting Artificial Atom, Phys. Rev. Lett. **104**, 163601 (2010).

[9] S. R. Sathyamoorthy, L. Tornberg, A. F. Kockum, B. Q. Baragiola, J. Combes, C. M. Wilson, T. M. Stace, and G. Johansson, Quantum Nondemolition Detection of a Propagating Microwave Photon, Phys. Rev. Lett. **112**, 093601 (2014).

[10] D. M. Toyli, A. W. Eddins, S. Boutin, S. Puri, D. Hover, V. Bolkhovsky, W. D. Oliver, A. Blais, and I. Siddiqi, Resonance Fluorescence from an Artificial Atom in Squeezed Vacuum, Phys. Rev. X **6**, 031004 (2016).

[11] Y.-X. Liu, H.-C. Sun, Z. Peng, A. Miranowicz, J. Tsai, and F. Nori, Controllable microwave three-wave mixing via a single three-level superconducting quantum circuit, Sci. Rep. **4**, 7289 (2014).

[12] P. Lähteenmäki, G. S. Paraoanu, J. Hassel, and P. J. Hakonen, Dynamical Casimir effect in a Josephson metamaterial, Proc. Natl. Acad. Sci. USA **110**, 4234 (2013).

[13] C. M. Wilson, G. Johansson, A. Pourkabirian, J. R. Johansson, T. Duty, F. Nori, and P. Delsing, Observation of the dynamical Casimir effect in a superconducting circuit, Nature (London) **479**, 376 (2011).

[14] D. S. Shapiro, A. A. Zhukov, W. V. Pogosov, and Yu. E. Lozovik, Dynamical Lamb effect in a tunable superconducting qubit-cavity system, Phys. Rev. A **91**, 063814 (2015).

[15] A. Yu. Dmitriev, R. Shaikhaidarov, V. N. Antonov, T. Hönigl-Decrinis, and O. V. Astafiev, Quantum wave mixing and visualisation of coherent and superposed photonic states in a waveguide, Nat. Commun. **8**, 1352 (2017).

[16] T. Hönigl-Decrinis, I. V. Antonov, R. Shaikhaidarov, V. N. Antonov, A. Yu. Dmitriev, and O. V. Astafiev, Mixing of coherent waves in a single three-level artificial atom, Phys. Rev. A **98**, 041801(R) (2018).

[17] A. Yu. Dmitriev, R. Shaikhaidarov, T. Hönigl-Decrinis, S. E. de Graaf, V. N. Antonov, and O. V. Astafiev, Probing photon statistics of coherent states by continuous wave mixing on a two-level system, Phys. Rev. A **100**, 013808 (2019).

[18] G. J. Milburn and D. F. Walls, Quantum nondemolition measurements via quantum counting, Phys. Rev. A **28**, 2646 (1983).

[19] D. F. Walls, M. J. Collet, and G. J. Milburn, Analysis of a quantum measurement, Phys. Rev. D **32**, 3208 (1985).

[20] C. W. Gardiner, *Quantum Noise* (Springer-Verlag, Berlin, 1991).

[21] Z. H. Peng, S. E. de Graaf, J. S. Tsai, and O. V. Astafiev, Tuneable on-demand single-photon source in the microwave range, Nat. Commun. **7**, 12588 (2016).

[22] P. Forn-Diaz, C. W. Warren, C. W. S. Chang, A. M. Vadiraj and C. M. Wilson, On-Demand Microwave Generator of Shaped Single Photons, Phys. Rev. Applied **8**, 054015 (2017).

[23] Yu Zhou, Zhihui Peng, Yuta Horiuchi, O. V. Astafiev, and J. S. Tsai, Tunable Microwave Single-Photon Source Based on Transmon Qubit with High Efficiency, Phys. Rev. Applied **13**, 034007 (2020).

[24] O. Astafiev, A. M. Zagoskin, A. A. Abdumalikov, Jr., Yu. A. Pashkin, T. Yamamoto, K. Inomata, Y. Nakamura, and J. S. Tsai, Resonance Fluorescence of a Single Artificial Atom, Science **327**, 840 (2010).

[25] W. M. Ruyten, Some analytical results for the fluorescence spectrum of a two-level atom in a bichromatic field, J. Opt. Soc. Am. B **9**, 1892 (1992).

[26] G. S. Agarwal, Yifu Zhu, Daniel J. Gauthier, and T. W. Mossberg, Spectrum of radiation from two-level atoms under intense bichromatic excitation, J. Opt. Soc. Am. B **8**, 1163 (1991).

[27] H. Freedhoff and Z. Chen, Resonance fluorescence of a two-level atom in a strong bichromatic field, Phys. Rev. A **41**, 6013 (1990).

[28] G. Breitenbach, S. Schiller, and J. Mlynek, Measurement of the quantum states of squeezed light, Nature (London) **387**, 471 (1997).

[29] C. W. Gardiner, Driving a Quantum System with the Output Field from Another Driven Quantum System, Phys. Rev. Lett. **70**, 2269 (1993).

[30] C. W. Gardiner and A. S. Parkins, Driving atoms with light of arbitrary statistics, Phys. Rev. A **50**, 1792 (1994).

[31] H. Ritsch and P. Zoller, Systems driven by colored squeezed noise: The atomic absorption spectrum, Phys. Rev. A **38**, 4657 (1988).

Correction: An affiliation has been added for the second author, necessitating renumbering of affiliations for the third author.